Петрология магматических и метаморфических комплексов

Выпуск 10

Материалы X Всероссийской конференции
с международным участием

27 ноября – 30 ноября 2018 года

Томск 2018

AN EXTENSIVE K-BENTONITE AS AN INDICATOR OF A SUPER-ERUPTION IN NORTHERN IBERIA 477 MY AGO

G. Gutiérrez-Alonso[1,2], J.C. Gutiérrez-Marco[3], J. Fernández-Suárez[3,4],
E. Bernárdez[5], F. Corfu[6], A. López-Carmona[2,4]

[1] Department of Geology, University of Salamanca, 33708 Salamanca, Spain (gabi@usal.es)
[2] Geology and Geography Department, Tomsk State University, Lenin Street 36, Tomsk 634050, Russian Federation.
[3] Instituto de Geociencias (CSIC, UCM), Severo Ochoa 7, 28040 Madrid, Spain.
[4] Department of Mineralogy and Petrology, Universidad Complutense, 28040, Madrid, Spain.
[5] Departamento de Geología, Universidad de Atacama, Copayapi 485, Copiapó, Chile
[6] Department of Geosciences, University of Oslo, PB1047 Blindern, 0316 Oslo, Norway.

*Zircon and monazite ID-TIMS U-Pb dating of four Lower Ordovician altered ash-fall tuff beds (K-Bentonites) in NW Iberia provided coetaneous ages of 477.5±1, 477±1.3 Ma, 477.2±1.1 Ma and 477.3±1 Ma, with a pooled concordia age of 477.2±0.74 Ma. A conservative estimation of the volume and mass of the studied K-bentonite beds (using data from the Cantabrian Zone) returns a minimum volume for the preserved deposits of ca. 37.5 km³ (Volcanic Explosivity Index - VEI = 6, Colossal). When considering other putative equivalent beds in other parts of Iberia and neighboring realms the volume of ejecta associated to this event would make it reach the Supervolcanic-Apocalyptic status (VEI=8, >1000 km3). Contrary to most cases of this kind of gargantuan eruption events, the studied magmatic event took place in relation to continental margin extension and thinning and not to plate convergence. We speculate that a geochronologically coincident large caldera event observed in the geological record of NW Iberia could be **ground zero** of this super-eruption.*

ОБШИРНЫЕ ОТЛОЖЕНИЯ К-БЕНТОНИТОВ КАК ИНДИКАТОР СУПЕРВЗРЫВА В СЕВЕРНОЙ ИБЕРИИ НА УРОВНЕ 477 МИЛЛИОНОВ ЛЕТ НАЗАД.

G. Gutiérrez-Alonso[1,2], J.C. Gutiérrez-Marco[3], J. Fernández-Suárez[3,4], E. Bernárdez[5],
F. Corfu[6], A. López-Carmona [2,4]

[1] Отдел геологии Саламанского университета, Испания
[2] Геолого-географический факультет Томского государственного университета,
[3] Институт геофизики (CSIC, UCM), Мадрид, Испания.
[4] Кафедра минералогии и петрологии, Университет Комплутенсе, Мадрид, Испания.
[5] Кафедра геологии, Университет Атакама, Копьяпо, Чили
[6] Кафедра геофизических исследований, Университет Осло, Норвегия.

Датировка U-Pb методом циркона и монацита (ID-TIMS) четырех нижнеордовикских измененных слоев туфа (К-бентониты) в северо-западной части провинции Иберия при условии, что реальные возрасты их формирования составляют 477,5 ± 1,3 млн. лет, 477,2 ± 1,1 млн. лет и 477,3 ± 1 млн лет , с объединенным конкордтаным возрастом 477,2 ± 0,74 млн. лет. Вероятное распространение массы изученных К-бентонитовых слоев подобных отложений Кантабрианской зоны позволяет оценить выделенного пеплового материала в объеме порядка 37,5 км³ (показатель взрывоопасности вулкана - VEI = 6, т.е. весьма колоссальный). Рассматривая другие предполагаемые эквивалентные слои в других частях Иберии и соседних регионах, объем выброса, связанный с этим событием, может достигнуть уровня супервулкана (VEI = 8,> 1000 км3), который мог определять существенные изменения органического мира на нашей планете. Вопреки большинству случаев такого рода гигантских извержений, проявление данного магматического события могло иметь место не только в режиме наращивания мощности земной коры при столкновении плит , но и при их дезинтеграции, т.е. в режиме проявления внутрипритной активности или проявления крупных изверженных провинций . Мы предполагаем, что геохронологически совпадающее крупное событие кальдеры, наблюдаемое в геологической летописи СЗ Иберии, может отражать один из главных этапов в эволюции Земли и её органического мира.

Introduction

Volcanic supereruptions (Rampino and Self, 1992) are contemplated to be those that discharge magma in excess of 10^{15} kg, commensurate to a volume of more than 450 km³ (Self, 2006; Sparks et al., 2005) in a relatively brief period of time (Mason et al., 2004; Miller and Wark, 2008) with a Volcanic Explosivity Index (VEI) (Newhall and Self, 1982) commonly over 8. These singular volcanic episodes appear to happen prompted by melt buoyancy (Malfait et al., 2014) with a worldwide prevalence ranging from 1.4 to 22 events/Ma (Mason et al., 2004), which should make them ample in the geological record.

Still, few such eruptions are noticed in the geological record on account of: i) the odds of preservation are scant as the deposits they generate are easily eroded and ii) even if the deposits are perpetuated, they are challenging to recognize and reconstruct once they have been altered, deformed, metamorphosed and dismembered by ensuing geological events. For instance, the last 45 My of Earth history preserve deposits caused by at least 45 supereruptions (Mason et al., 2004) while in the Ordovician period, covering the same time span (*ca.* 42 My), only two supereruptions, preserved as altered volcanic ash-fall deposits (K-bentonites), have been diagnosed so far (Huff, 2008; Huff et al., 1992;

Huff et al., 2010; Huff et al., 1996; Sell et al., 2013).

In this paper we target on the Lower Ordovician ash-fall deposits found in northern Iberia and contribute geological and geochronological data, as well as arguments, that support the idea that the deposits were the result of one super-eruption that occured in the rifted and extended northern margin of west Gonwana during Floian times. This event took place at a passive margin while it was being thinned and extended during the initial phases of the Rheic Ocean opening (see Murphy et al., 2006).

Geological setting

The Lower Paleozoic succession in northwest Iberia is characterized by the profusion of long-lived magmatism which is expressed mainly by the so called "Ollo de Sapo" plutonic and volcanic episode extending in age between ca. 490 and 465 Ma, with a maximum at ca. 477 Ma, Fig. 1C (Montero et al., 2009b; Talavera et al., 2013).

Within the Cantabrian Zone (CZ), this event is represented by alkaline basalts and volcaniclastic rocks interbedded within Upper Cambrian and Lower Ordovician strata (Gallastegui et al., 1992; Heinz et al., 1985; Loeschke and Zeidler, 1982) together with an extensive K-bentonite (Pedroso-Valverdín bed) within the Lower Ordovician succession (Fig. 1A), (García-Ramos et al., 1984) which is the main object of this study. Ash-tuff beds correlatable with the Pedroso-Valverdín bed also crop out in other parts of Iberia as the Iberian Ranges (IR) (Tranquera bed, Fig. 1A (Alvaro et al., 2008) and in the Westasturian-Leonese Zone (WALZ) (Villa et al., 2004).

The Lower Ordovician shallow-water siliciclastic succession hosting the studied ash beds is widely exposed in Western Europe (e.g. Alvaro et al., 2008; Aramburu, 1989; Aramburu and García-Ramos, 1993) and its provenance established through detrital zircons (Shaw et al., 2014). The Pedroso-Valverdín K-bentonite bed (Fig. 1A) extends over the whole CZ (Fig. 1A) more than 1800 km[2] with a thickness between 45 and 80 cm (Aramburu, 1989). It is interpreted as an altered ash-fall tuff ("kaolinite tonstein" Aramburu, 1989; García-Ramos et al., 1984). The upper and lower contacts are very sharp and the massive ash-fall apparently did not affect the population structure and the development of the benthic communities, which attained a rapid recovery and re-colonization of the shallow marine environment in a way similar to that observed in other Ordovician and modern ash-falls (Huff et al., 1992; Kuhnt et al., 2005).

The origin of the Lower Ordovician magmatism in the studied sector of the Gondwanan margin (Fig. 1B) is interpreted to be related to extension, linked to the undocking of Avalonia (Murphy et al., 2006).

The three new studied samples plus a sample from Mina Conchita (Fig. 1A) (Gutiérrez Alonso et al., 2007), were collected in the Cantabrian Zone. The K-bentonite samples contained mainly zircon, monazite and pyrite as heavy minerals, which is indicative of limited reworking in the sedimentary environment, in contrast to other K-bentonites with the heavy mineral association zircon-tourmaline-rutile, which is a common feature of highly reworked bentonites in which the proportion of *remanié* zircons is usually high.

Geochronology

U-Pb ID-TIMS analytical method

U-Pb analytical work was conducted at the Department of Geosciences, University of Oslo, Norway. Isotope data and details of each analyzed fraction are given in Table 1. The analytical procedure for zircon and monazite analyses is also described in Gutiérrez-Alonso et al., (2016). U-Pb data are shown as Wetherill concordia plots in Fig. 1D.

Results

For sample **AST-1** (Gutierrez-Alonso et al., 2007) we use the published age of 477.5±1 Ma (Concordia age of 6 concordant and overlapping analyses on single abraded grains, Fig. 1D.4).

For the 3 new samples selected for this study (LBL, GRADO and TUN-194) the best U-Pb age estimate has been calculated as described below:

Sample LBL: 11 zircon and 3 monazite fractions were analysed (see details in Table 1). Of the 11 zircon analyses, 5 are discordant and are no longer considered in age calculations. The six concordant analyses (Table 1) yield a concordia age of **477±1.3** Ma (Fig. Fig. 1 D.1). This age is within error of the weighted average of the $^{207}Pb/^{235}U$ age (chosen because of reverse discordance, see (Scharer, 1984) of the 3 monazite analyses (478±2.7 Ma) from the same sample.

Sample GRADO: Nine zircon and one monazite fractions were analysed. Of the 9 zircon fractions 3 are >5% discordant and were not considered for age calculation. With the remaining analyses (discordance between -0.2% and 3.8%, Table 1) we calculated an upper intercept age anchored at 0±10 Ma (Fig. 1D.2) of 477.2±2.3 Ma, and a concordia age with the two top analyses (Fig. 1D.2) of **477.2±1.1 Ma**. This age is within error of the $^{207}Pb/^{235}U$ age of the reversely discordant monazite analysis (478±1 Ma).

Sample TUN-194: 10 zircon and one monazite analyses were performed on fractions separated from this sample. Of the 10 zircon analyses, 3 were discordant and are not considered in the age calculation (Table 1). The remaining 7 concordant zircon analyses yield a concordia age of **477.3±1 Ma** (Fig. 1D.3), within error of the $^{207}Pb/^{235}U$ age of the reversely discordant monazite analysis (479±1 Ma).

Within the precision of the U-Pb analyses in this study, it can be stated that the four samples are coeval and possibly belong to the same volcanic event. The best age assesment for the volcanic event can be gathered by the pooled 21 concordant analyses from the four samples described above (Fig. 1), yielding a concordia age of **477.2±0.74 Ma** which concurs with the Tremadocian-Floian boundary (477.7±1.4 Ma, (Gradstein et al., 2012). This concordia age is consistent with the age obtained using the TuffZirc algorithm of Isoplot 3.7 (Ludwig, 2009) which provides an age of 477.5 +0.75/-1.1 Ma using the $^{206}Pb/^{238}U$ ages of the same set of 21 concordant analyses.

All the monazite analyses show reverse discordance and their average $^{207}Pb/^{235}U$ age is 1 to 2 Myr older than the concordia age of the zircons in the same samples (Table 1). Since the closure temperature of monazite for the U-Pb system and its Pb retentivity can be higher than those of zircon (e.g. (Cherniak et al., 2004) the monazite ages could represent an older pre-eruptive stage and the zircon be closer to the eruption stage. In any case, this observation does not challenge the inference that all the studied samples are coeval at the level of precision achieved in this study.

Volume and mass calculation

Given the aerial extension and the thickness of the studied K-bentonite, and given the geochronological evidence aforementioned for its assignment to a single event, we can attempt to rconstruct its initial mass and volume to grade the magnitude of the volcanic event. For this scope, we have reconstructed the Variscan deformation by unfolding the Cantabrian Arc (Fig. 1A) and restoring the shortening caused by the Variscan thrusting and folding (Fig. 1A). Upon a conservative restoration considering the minimum shortening during the late Devonian-Carboniferous Variscan orogeny of the different units involved (ranging from 100% in the foreland to more than 200% in the hinterland), the areal extent of the K-bentonite bed, based on the locations of the known outcrops

in the Cantabrian Zone may have exceeded ca. 15000 km^2, and 100000 km^2 when considering the correlatable beds in the proximal IR and WALZ and Central Iberian Zone (CIZ, Fig. 1A). The thickness of the studied tonstein shows a steady thinning trend from the westernmost outcrops in the CZ, where the thickness attains up to 80 cm. In the surrounding regions, thickness estimations should be taken cautiously as the tuff beds have suffered internal strain and their thickness (from a few centimeters to several meters) should be treated as a minimum.

A conservative evaluation of the volume and mass of the studied K-bentonite (using exclusively the Cantabrian Zone data, Fig. 1A) done with the Weibull fit method (Bonadonna and Costa, 2012) provides a volume for the preserved deposits of ca. 37.5 km^3 (Volcanic Explosivity Index - VEI = 6, Colossal) which corresponds to a mass of ca. $8.3 \cdot 10^{13}$ kg using a measured mean density value of 2200 kg/m^3.

When considering other outcrops in northern Iberia which can be likely correlated with the dated K-bentonites, these values increase to ca. 400 km^3 (VEI = 7, Mega-colossal) which would correspond to a mass of ca. $9 \cdot 10^{14}$ kg. These occurrences may be linked to the large magmatic event regionally known as "Ollo de Sapo" (i.e. Talavera et al., 2013, and references therein) whose main age (including many volcanic rocks and their plutonic correlatives) peaks at ca. 477 Ma (Fig. 1C). Furthermore, the studied K-bentonites are coeval with the intrusion of a peralkaline ring complex attributed to a large caldera event in NW Iberia (Fig. 1A, (Diez Fernandez et al., 2012; Diez Fernandez and Martinez Catalan, 2009; Montero et al., 2009a). Whether or not this caldera was the main source of the dated ash-fall beds (and their correlatives) cannot be ascertained with available geological data.

Discussion

The data presented document the first described occurrence of a gigantic volcanic ash-fall/event in the Lower Ordovician. Such an event has only been recognized in the Upper Ordovician (ca. 454 Ma), (Fig. 1B) (Huff, 2008; Huff et al., 1998; Sell et al., 2013).

The apparent coeval nature. same U-Pb zircon age within a ca. 1My uncertainty, of the studied samples present in the same stratigraphic position is an argument for a large eruptive episode in Gondwana ca. 477 My ago. The CZ is the domain where the K-bentonite layer is better preserved but its areal extension should have been much larger; covering most of Iberia and adjacent realms. Preservation of ash-fall beds (ultimately occurring as K-bentonite layers) requires lack of sedimentary reworking and the existence of large basins. In Iberia, the Lower Ordovician stratigraphic record is interpreted to be restricted to relatively small domains due to basin fragmentation and large emerged areas, especially in the southern part of the CIZ (Sá et al., 2013). Given that in northern Iberia there is a continuous sedimentary record for the Lower Ordovician, the best preservation occurs in it and the studied K-bentonite is ubiquitously recognized in areas lacking metamorphism and internal strain.

The large amount of igneous rocks coetaneous with the studied K-bentonite layer found in Iberia and neighboring areas (see Fig. 1C) is consistent with the notion that the K-bentonite could have been much more extensive than what is preserved in the Cantabrian Zone. Because of the fragmented stratigraphic record, it is not possible to appraise the real size of the volcanic episode recorded in NW Iberia. Still, when considering other possible equivalent areas in Iberia and neighboring terranes (i.e. Armorica, Sardinia, etc. (Bonjour and Odin, 1989), the volume of ejecta related to this event would make it grasp the Supervolcanic-Apocalyptic category (VEI=8, >1000 km3).

References

1. Alvaro, J. J., Ezzouhairi, H., Ribeiro, M. L., Ramos, J. F., and Sola, A. R., 2008, Early Ordovician volcanism in the Iberian Chains (NE Spain) and its influence on the preservation of shell concentrations: Bulletin De La Societe Geologique De France, v. 179, no. 6, p. 569-581.

2. Aramburu, C., 1989, El Cambro-Ordovícico de la Zona Cantábrica (NO de España) [PhD: Oviedo University, 530 p.

3. Aramburu, C., and García-Ramos, J. C., 1993, La sedimentación Cambro-Ordovícica en la Zona Cantábrica (NO de España): Trabajos de Geología, Universidad de Oviedo, v. 19, p. 45-73.

4. Bonadonna, C., and Costa, A., 2012, Estimating the volume of tephra deposits: A new simple strategy: Geology, v. 40, no. 5, p. 415-418.

5. Bonjour, J. L., and Odin, G. S., 1989, Recherche sur les volcanoclastites des Séries Rouges Initiales en presqu'île de Crozon: premier âge radiométrique de l'Arénig: Géologie de la France, v. 4, p. 3-8.

6. Cherniak, D. J., Watson, E. B., Grove, M., and Harrison, T. M., 2004, Pb diffusion in monazite: A combined RBS/SIMS study: Geochimica Et Cosmochimica Acta, v. 68, no. 4, p. 829-840.

7. Diez Fernandez, R., Castineiras, P., and Gomez Barreiro, J., 2012, Age constraints on Lower Paleozoic convection system: Magmatic events in the NW Iberian Gondwana margin: Gondwana Research, v. 21, no. 4, p. 1066-1079.

8. Diez Fernandez, R., and Martinez Catalan, J. R., 2009, 3D Analysis of an Ordovician igneous ensemble: A complex magmatic structure hidden in a polydeformed allochthonous Variscan unit: Journal of Structural Geology, v. 31, no. 3, p. 222-236.

9. Gallastegui, G., Aramburu, C., Barba, P., Fernandez, L. P., and Cuesta, A., 1992, Volcanism of the Lower Paleozoic in the Cantabrian Zone (Northwestern Spain): Iberian and Ibero-American Lower Paleozoic, p. 435-452.

10. García-Ramos, J. C., Aramburu, C., and Brime, C., 1984, Kaolin tonstein of volcanic ash origin in the Lower Ordovician of the Cantabrian Mountains (NW Spain): Trabajos de Geología, Universidad de Oviedo, v. 14, p. 27-33.

11. Gradstein, F. M., Ogg, J. G., Schmitz, M. D., and Ogg, G. M., 2012, The Geological Time Scale 2012 Amsterdam, Elsevier, p. 1144.

12. Gutierrez-Alonso, G., Fernández-Suárez, J., Gutiérrez-Marco, J. C., Corfu, F., Murphy, J. B., and Suárez, M., 2007, U-Pb depositional age for the upper Barrios Formation (Armorican Quartzite facies) in the Cantabrian zone of Iberia: Implications for stratigraphic correlation and paleogeography, *in* Linnemann, U., Nance, R. D., Kraft, P., and Zulauf, G., eds., The Evolution of the Rheic Ocean: From Avalonian-Cadomian Active Margin to Alleghenian-Variscan Collision, Volume 423: Boulder (USA), Geological Society of America, p. 287-296.

13. Gutierrez-Alonso, G., Gutiérrez-Marco, J.C., Fernández-Suárez, J., Bernardez, E., Corfu, F., 2016. Was there a super-eruption on the Gondwanan coast 477 Ma ago?: Tectonophysics, v. 681, p. 85-94.

14. Heinz, W., Loeschke, J., and Vavra, G., 1985, Phrestomagmatic volcanism during the Ordovivian of the Cantabrian Mountains (NW Spain): Geologische Rundschau, v. 74, no. 3, p. 623-639.

15. Huff, W. D., 2008, Ordovician K-bentonites: Issues in interpreting and correlating ancient tephras: Quaternary International, v. 178, p. 276-287.

16. Huff, W. D., Bergstrom, S. M., and Kolata, D. R., 1992, Gigantic Ordovician volcanic ash fall in North America and Europe - Biological, Tectonomagmatic, and event-stratigraphic significance: Geology, v. 20, no. 10, p. 875-878.

17. Huff, W. D., Bergstrom, S. M., and Kolata, D. R., 2010, Ordovician explosive volcanism, *in* Finney, S. C., and Berry, W. B. N., eds., The Ordovician Earth System, Volume Geological Society of America Special Paper 466, Geological Society of America, p. 13-28.

18. Huff, W. D., Bergstrom, S. M., Kolata, D. R., Cingolani, C. A., and Astini, R. A., 1998, Ordovician K-bentonites in the Argentine Precordillera: relations to Gondwana margin evolution: Proto-Andean Margin of Gondwana, no. 142, p. 107-126.

19. Huff, W. D., Kolata, D. R., Bergstrom, S. M., and Zhang, Y. S., 1996, Large-magnitude Middle Ordovician volcanic ash falls in North America and Europe: Dimensions, emplacement and post-emplacement characteristics: Journal of Volcanology and Geothermal Research, v. 73, no. 3-4, p. 285-301.

20. Kuhnt, W., Hess, S., Holbourn, A., Paulsen, H., and Salomon, B., 2005, The impact of the 1991 Mt. Pinatubo eruption on deep-sea foraminiferal communities: A model for the Cretaceous-Tertiary (K/T) boundary?: Palaeogeography Palaeoclimatology Palaeoecology, v. 224, no. 1-3, p. 83-107.

21. Loeschke, J., and Zeidler, N., 1982, Early Paleozoic sills in the Cantabrian Mountains (Spain) and their geotectonic environment., Neues Jahrbuch für Geologie und Paläontologie, Monatshefte p. 419-439.

22. Ludwig, K. R., 2009, Isoplot v. 3.71: a geochronological toolkit for Microsoft Excel, Volume Special Publication: California (USA), Berkeley Geochronology Center.

23. Malfait, W. J., Seifert, R., Petitgirard, S., Perrillat, J.-P., Mezouar, M., Ota, T., Nakamura, E., Lerch, P., and Sanchez-Valle, C., 2014, Supervolcano eruptions driven by melt buoyancy in large silicic magma chambers: Nature Geoscience, v. 7, no. 2, p. 122-125.

24. Mason, B. G., Pyle, D. M., and Oppenheimer, C., 2004, The size and frequency of the largest explosive eruptions on Earth: Bulletin of Volcanology, v. 66, no. 8, p. 735-748.

25. Miller, C. F., and Wark, D. A., 2008, Supervolcanoes and their explosive supereruptions: Elements, v. 4, no. 1, p. 11-15.

26. Montero, P., Bea, F., Corretge, L. G., Floor, P., and Whitehouse, M. J., 2009a, U-Pb ion microprobe dating and Sr and Nd isotope geology of the Galineiro Igneous Complex A model for the peraluminous/peralkaline duality of the Cambro-Ordovician magmatism of Iberia: Lithos, v. 107, no. 3-4, p. 227-238.

27. Montero, P., Talavera, C., Bea, F., Lodeiro, F. G., and Whitehouse, M. J., 2009b, Zircon Geochronology of the Ollo de Sapo Formation and the Age of the Cambro-Ordovician Rifting in Iberia: Journal of Geology, v. 117, no. 2, p. 174-191.

28. Murphy, J. B., Gutierrez-Alonso, G., Nance, R. D., Fernandez-Suarez, J., Keppie, J. D., Quesada, C., Strachan, R. A., and Dostal, J., 2006, Origin of the Rheic Ocean: Rifting along a Neoproterozoic suture?: Geology, v. 34, no. 5, p. 325-328.

29. Newhall, C. G., and Self, S., 1982, The Volcanic Explosivity Index (VEI) - an estimate of explosive magnitude for historical volcanism: Journal of Geophysical Research-Oceans and Atmospheres, v. 87, no. NC2, p. 1231-1238.

30. Rampino, M. R., and Self, S., 1992, Volcanic winter and accelerated glaciation following the Toba super-eruption: Nature, v. 359, no. 6390, p. 50-52.

31. Scharer, U., 1984, The effect of initial Th-230 disequilibrium on young U-Pb ages- The Makalu case, Himalaya: Earth and Planetary Science Letters, v. 67, no. 2, p. 191-204.

32. Self, S., 2006, The effects and consequences of of very large explosive volcanic eruptions: Philosophical Transactions of the Royal Society, v. A364.

33. Sell, B., Ainsaar, L., and Leslie, S., 2013, Precise timing of the Late Ordovician (Sandbian) super-eruptions and associated environmental, biological, and climatological events: Journal of the Geological Society, v. 170, no. 5, p. 711-714.

34. Shaw, J., Gutierrez-Alonso, G., Johnston, S. T., and Galan, D. P., 2014, Provenance variability along the Early Ordovician north Gondwana margin: Paleogeographic and tectonic implications of U-Pb detrital zircon ages from the Armorican Quartzite of the Iberian Variscan belt: Geological Society of America Bulletin, v. 126, no. 5-6, p. 702-719.

35. Sparks, R. S. J., Self, S., Grattan, J. P., Oppenheimer, C., Pyle, D. M., and Rymer, H., 2005, Supereruptions: global effects and future threats.: The Geological Society, London.

36. Sá, A. A., Gutiérrez-Marco, J. C., Meireles, C. A. P., García-Bellido, C., and Rábano, I., 2013, A revised correlation of Lower Ordovician sedimentary rocks in the Central Iberian Zone (Portugal and Spain), *in* R.B. Rocha, J. P., C. Kulberg, S. Finney, ed., Strati 2013, at the cutting edge of Stratigraphy: Lisbon, Springer Geology Series, p. 441-446.

37. Talavera, C., Montero, P., Bea, F., Gonzalez Lodeiro, F., and Whitehouse, M., 2013, U-Pb Zircon geochronology of the Cambro-Ordovician metagranites and metavolcanic rocks of central and NW Iberia: International Journal of Earth Sciences, v. 102, no. 1, p. 1-23.

38. Villa, L., Corretgé, L. G., Arias, D., and Suárez, O., 2004, Los depósitos sin-eruptivos del Paleozoico inferior del área de Lago Fontarón (Lugo, España): Trabajos de Geología, v. 24, p. 185-205.
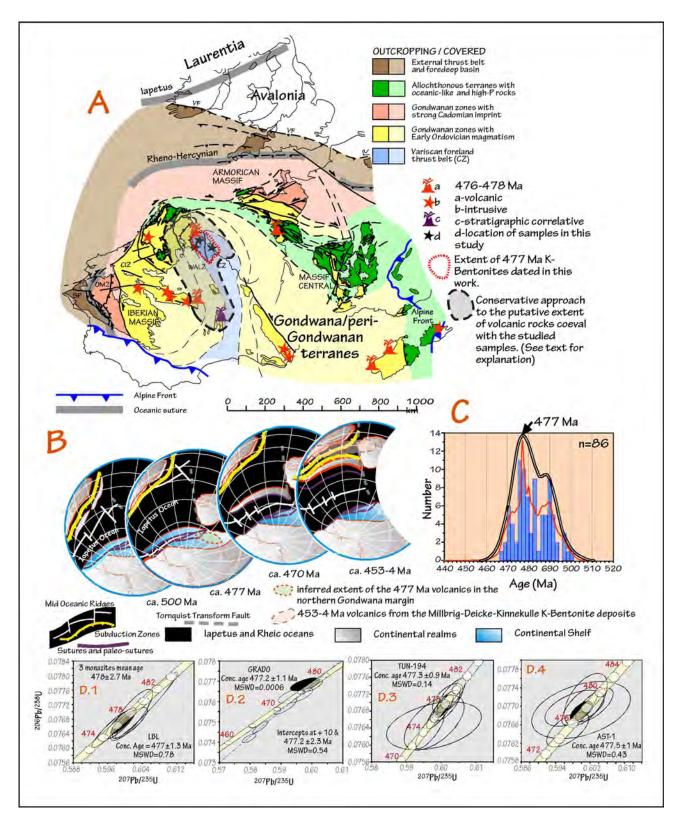
Figure 1.- (A) Paleogeographic reconstruction of Western Europe in early Mesozoic times with the sample locations, the known outcrops of ca. 477 Ma intrusive and extrusive rocks and the extension of the recognized ash-tuff layer studied as well as the conservatively considered extension for a more interpretative volume calculation. (B) Early Paleozoic reconstruction of the Rheic Ocean opening and the origin and putative extension of the super eruptions identified in Ordovician times. (C) Histogram, Probability Density Diagram, and Kernel analysis plot of the available intrusive and extrusive age data between 465 and 500 Ma. in western Europe, which reveals a significant maxima at 477 Ma, coeval with the age of the identified ash-tuff layer. (D) Wetherill concordia plots of the studied samples. (Modified from Gutiérrez-Alonso et al., 2016)

Table 1.- U–Pb data from the studied sample.

Properties (1)	Weight [ug] (2)	U [ppm] (2)	Th/U (3)	Pbc [pg] (4)	206/204 (5)	207/235 (6)	2 sigma [abs] (6)	206/238 (6)	2 sigma [abs] (6)	rho	207/206 (6)	2 sigma [abs] (6)	206/238 (6)	2 sigma [abs] (6)	207/235 (6)	2 sigma [abs] (6)	207/206 (6)	2 sigma [abs] (6)
LBL (N42°50'57.22" W005°51'57.74")																		
Z sp [1]	1	2127	0.19	1.3	10612	0.9018	0.0052	0.10247	0.00058	0.98	0.06383	0.00008	628.9	3.4	652.7	2.8	735.9	2.5
Z tip [1]	1	823	0.21	1.2	3653	0.7057	0.0095	0.08648	0.00115	0.95	0.05918	0.00026	534.7	6.8	542.2	5.7	573.7	9.5
Z tip el p [1]	1	652	0.28	1.0	3565	0.6637	0.0034	0.08331	0.00037	0.89	0.05778	0.00013	515.9	2.2	516.9	2.1	521.4	5.1
Z lp tips [8]	2	518	0.15	1.1	4626	0.6049	0.0058	0.07719	0.00074	0.97	0.05684	0.00013	479.3	4.4	480.3	3.7	485.1	5.2
Z lp [4]	11	319	0.17	2.1	7924	0.6015	0.0040	0.07693	0.00057	0.83	0.05671	0.00024	477.8	3.4	478.2	2.5	480.2	9.2
Z lp [9]	13	277	0.18	2.0	8633	0.5991	0.0016	0.07672	0.00019	0.85	0.05664	0.00008	476.5	1.1	476.7	1.0	477.5	3.1
Z lp fr [1]	1	1255	0.11	3.6	1689	0.6011	0.0033	0.07671	0.00035	0.83	0.05684	0.00018	476.4	2.1	478.0	2.1	485.3	6.8
Z lp fr [1]	2	451	0.41	0.9	4592	0.5990	0.0030	0.07669	0.00030	0.86	0.05654	0.00014	476.3	2.1	476.6	1.9	477.7	5.6
Z lp tip[1]	1	1218	0.15	1.2	4890	0.5965	0.0034	0.07652	0.00041	0.93	0.05654	0.00012	475.3	2.4	475.0	2.2	473.5	4.7
Z lp [1]	6	149	0.25	2.6	1672	0.5915	0.0024	0.07556	0.00020	0.59	0.05677	0.00019	469.6	1.2	471.8	1.5	482.8	7.2
Z lp [1]	11	100	0.19	1.7	2988	0.5869	0.0020	0.07488	0.00019	0.69	0.05685	0.00014	465.5	1.1	468.9	1.3	485.7	5.5
MON NA [8]	18	900	33.08	10.6	7433	0.6045	0.0015	0.07760	0.00016	0.94	0.05656	0.00005	481.8	1.0	480.1	0.9	471.9	1.9
MON [1]	3	559	34.31	4.5	1815	0.5981	0.0022	0.07732	0.00022	0.75	0.05611	0.00013	480.1	1.3	476.0	1.4	456.6	5.3
MON [4]	4	261	30.26	3.4	1492	0.6019	0.0025	0.07739	0.00020	0.60	0.05641	0.00018	480.5	1.2	478.4	1.6	468.6	7.2
TUN 194 (N043°27'49.70" W005°08'41.11")																		
Z sp [1]	<1	>410	0.19	0.8	9917	8.9681	0.0358	0.30603	0.00116	0.98	0.21253	0.00019	1721.2	5.7	2334.8	3.6	2925.0	1.4
Z sp [1]	1	827	0.21	1.0	6447	1.5837	0.0051	0.12006	0.00037	0.89	0.09567	0.00014	730.9	2.1	963.8	2.0	1541.3	2.8
Z lp [1]	<1	>670	0.13	1.5	2240	0.6029	0.0033	0.07717	0.00033	0.79	0.05666	0.00019	479.2	2.0	479.1	2.1	478.4	7.4
Z lp [1]	<1	>620	0.09	3.3	923	0.6019	0.0036	0.07711	0.00028	0.60	0.05661	0.00027	478.8	1.7	478.4	2.3	476.4	10.4
Z lp [1]	1	463	0.17	1.1	2068	0.6015	0.0032	0.07694	0.00029	0.72	0.05670	0.00021	477.8	1.8	478.2	2.0	479.9	8.1
Z lp [1]	<1	>680	0.14	1.1	2966	0.5997	0.0031	0.07679	0.00033	0.84	0.05664	0.00016	476.9	2.0	477.0	2.0	477.4	6.2
Z lp [1]	<1	>420	0.08	5.3	408	0.5935	0.0059	0.07666	0.00033	0.51	0.05615	0.00048	476.2	2.0	473.1	3.7	458.2	18.7
Z lp [1]	1	95	0.10	0.7	712	0.5980	0.0070	0.07653	0.00053	0.58	0.05667	0.00054	475.4	3.2	476.0	4.4	478.9	20.9
Z lp [1]	<1	>100	0.13	1.3	379	0.5980	0.0111	0.07646	0.00046	0.37	0.05672	0.00098	474.9	2.8	475.9	7.0	480.9	37.6
Z lp [1]	<1	>530	0.12	1.1	2309	0.5968	0.0034	0.07634	0.00035	0.79	0.05669	0.00020	474.3	2.1	475.2	2.1	479.6	7.6
MON NA [8]	12	1168	27.93	5.8	11692	0.6028	0.0014	0.07736	0.00016	0.95	0.05652	0.00004	480.3	1.0	479.0	0.9	472.8	1.7
GRADO (N43°24'10.54" W006°02'27.05")																		
Z lp [1]	1	521	0.51	1.7	2740	1.9436	0.0070	0.14398	0.00047	0.85	0.09791	0.00018	867.1	2.6	1096.2	2.4	1584.7	3.5
Z lp-flat fr [1]	6	432	0.13	17.0	774	0.6355	0.0028	0.07896	0.00020	0.54	0.05837	0.00022	489.9	1.2	499.5	1.8	543.8	8.2
Z lp-flat fr [9]	1	1005	0.33	10.0	4848	0.5803	0.0052	0.07397	0.00065	0.97	0.05690	0.00013	460.0	3.9	464.7	3.3	487.7	5.0
Z lp [1]	<1	>380	0.48	1.4	1311	0.5977	0.0038	0.07685	0.00026	0.63	0.05641	0.00028	477.3	1.5	475.8	2.4	468.4	11.1
Z lp [1]	8	149	0.32	2.3	2528	0.6003	0.0026	0.07679	0.00024	0.77	0.05670	0.00016	476.9	1.4	477.4	1.6	479.7	6.1
Z lp[1]	<1	>440	0.21	1.9	1111	0.5946	0.0045	0.07630	0.00033	0.62	0.05652	0.00034	474.0	2.0	473.8	2.9	472.8	13.1
Z lp-flat fr [1]	<1	>320	0.12	0.6	2799	0.5913	0.0030	0.07578	0.00032	0.80	0.05660	0.00017	470.9	1.9	471.7	1.9	475.9	6.7
Z lp [18]	6	289	0.17	3.7	2225	0.5798	0.0018	0.07420	0.00018	0.75	0.05667	0.00012	461.4	1.1	464.3	1.2	478.8	4.6
Z lp [1]	3	505	0.15	1.0	6835	0.5833	0.0021	0.07475	0.00025	0.89	0.05660	0.00009	464.7	1.5	466.6	1.3	476.0	3.6
MON NA [8]	14	364	34.35	4.2	5875	0.6015	0.0017	0.07727	0.00020	0.90	0.05646	0.00007	479.8	1.2	478.2	1.1	470.7	2.7
AST-1, Mina Conchita (Gutiérrez Alonso et al., 2007) (N43°19'25.7" W006°18'0.07")																		
Z lp [1]	5	127	0.14	1.9	1623	0.6030	0.0035	0.07703	0.00030	0.69	0.05677	0.00024	478.4	1.8	479.1	2.8	482.6	9.4
Z lp [1]	4	152	0.22	2.9	1004	0.5968	0.0040	0.07650	0.00031	0.63	0.05658	0.00029	475.2	1.9	475.2	3.2	475.4	11.4
Z lp [1]	4	143	0.22	7.3	397	0.5984	0.0056	0.07696	0.00032	0.53	0.05640	0.00045	477.9	.2	476.2	4.5	468.0	17.6
Z lp [1]	6	165	0.19	2.9	1675	0.6010	0.0040	0.07715	0.00046	0.56	0.05650	0.00034	479.1	2.9	477.9	3.2	472.0	13.3
Z lp [1]	4	78	0.29	5.4	298	0.5999	0.0093	0.07692	0.00081	0.39	0.05656	0.00050	477.7	3.1	477.2	7.4	474.6	31.3
Z lp [1]	5	84	0.30	4.2	1951	0.5996	0.0034	0.07701	0.00034	0.72	0.05647	0.00022	478.2	2.1	477.0	2.7	471.0	8.7

1) Z = zircon; MON = monazite; all euhedral clear grains; sp= short prismatic; lp = long prismatic; el = elongated; fr = fragment, broken prism; p = pink; NA = not air abraded, all other grains abraded; [1] number of grains in fractions; **Bold** indicates analyses considered in the age calculation

(2) concentration better than 10%, except for grains of 1-2 ug where uncertainty is up to 50%

(3) Th/U model ratio inferred from 208/206 ratio and age of sample

(4) Pbc= total amount of common Pb (initial + blank)

(5) raw data corrected for fractionation

(6) corrected for fractionation, spike, blank and initial common Pb; error calculated by propagating the main sources of uncertainty; initial common Pb corrected using Stacey & Kramers (1975) model compositions